

Investigation of magnetic domain evolutions and microstructural changes in Pr-Dy-Cu modified Nd-Fe-B magnets

Peng Shen(沈鹏), Hui-Dong Qian(千辉东), Jingzhi Han(韩景智), Tao Liu(刘涛), Zhen Yan(阎震), Ming Ji(姬明), Lei Zhou(周磊), Weiqiang Liu(刘卫强), Shunquan Liu(刘顺荃), Wenyun Yang(杨文云), Yan Li(李岩)5, Huihui Cao(曹慧慧), Ming Yue(岳明), Jinbo Yang(杨金波), and Yingchang Yang(杨应昌)

Citation: Chin. Phys. B, 2025, 34 (**8**): 087503. DOI: 10.1088/1674-1056/adda0c
http://cpb.iphy.ac.cn; http://iopscience.iop.org/cpb

What follows is a list of articles you may be interested in

Cu-doped nanocomposite $Pr_2Fe_{14}B/\alpha$-Fe ribbons with high $(BH)_{max}$

Mehran Khan Alam, Shahzab Raza, Chengyong Gao(高成勇), Guangbing Han(韩广兵), and Shishou Kang(康仕寿)
Chin. Phys. B, 2024, 33 (**12**): 127504. DOI: 10.1088/1674-1056/ad8cba

Optimization of the grain boundary diffusion process by doping gallium and zirconium in Nd-Fe-B sintered magnets

Zhiteng Li(李之藤), Haibo Xu(徐海波), Feng Liu(刘峰), Rongshun Lai(赖荣舜), Renjie Wu(武仁杰), Zhibin Li(李志彬), Yangyang Zhang(张洋洋), and Qiang Ma(马强)
Chin. Phys. B, 2023, 32 (**10**): 107503. DOI: 10.1088/1674-1056/acd61f

Effects of post-sinter annealing on microstructure and magnetic properties of Nd-Fe-B sintered magnets with Nd-Ga intergranular addition

Jin-Hao Zhu(朱金豪), Lei Jin(金磊), Zhe-Huan Jin(金哲欢), Guang-Fei Ding(丁广飞), Bo Zheng(郑波), Shuai Guo(郭帅), Ren-Jie Chen(陈仁杰), and A-Ru Yan(闫阿儒)
Chin. Phys. B, 2021, 30 (**6**): 067503. DOI: 10.1088/1674-1056/abddad

Progress in recycling of Nd-Fe-B sintered magnet wastes

Ming Yue(岳明), Xiaowen Yin(尹小文), Weiqiang Liu(刘卫强), Qingmei Lu(路清梅)
Chin. Phys. B, 2019, 28 (**7**): 077506. DOI: 10.1088/1674-1056/28/7/077506

Magnetic properties of misch-metal partially substituted Nd-Fe-B magnets sintered by dual alloy method

Jie-Fu Xiong(熊杰夫), Rong-Xiang Shang(商荣翔), Yan-Li Liu(刘艳丽), Xin Zhao(赵鑫), Wen-Liang Zuo(左文亮), Feng-Xia Hu(胡凤霞), Ji-Rong Sun(孙继荣), Tong-Yun Zhao(赵同云), Ren-Jie Chen(陈仁杰), Bao-Gen Shen(沈保根)
Chin. Phys. B, 2018, 27 (**7**): 077504. DOI: 10.1088/1674-1056/27/7/077504

Investigation of magnetic domain evolutions and microstructural changes in Pr–Dy–Cu modified Nd–Fe–B magnets

Peng Shen(沈鹏)[1], Hui-Dong Qian(千辉东)[1,†], Jingzhi Han(韩景智)[1,‡], Tao Liu(刘涛)[2], Zhen Yan(闫震)[3], Ming Ji(姬明)[4], Lei Zhou(周磊)[2], Weiqiang Liu(刘卫强)[4], Shunquan Liu(刘顺荃)[1], Wenyun Yang(杨文云)[1], Yan Li(李岩)[5], Huihui Cao(曹慧慧)[3], Ming Yue(岳明)[4], Jinbo Yang(杨金波)[1,2], and Yingchang Yang(杨应昌)[1]

[1] *Institute of Condensed Matter and Material Physics, School of Physics, Peking University, Beijing* 100871, *China*
[2] *Advanced Technology & Materials Co., Ltd., Beijing* 100081, *China*
[3] *Rare Earth Advanced Materials Technology Innovation Center, Inner Mongolia Northern Rare Earth Advanced Materials Technology Innovation Co., Ltd., Baotou* 014030, *China*
[4] *Faculty of Materials and Manufacturing, Key Laboratory of Advanced Functional Materials, Ministry of Education of China, Beijing University of Technology, Beijing* 100124, *China*
[5] *Inner Mongolia University of Science & Technology, Baotou* 014010, *China*

(Received 19 March 2025; revised manuscript received 6 May 2025; accepted manuscript online 19 May 2025)

The enhancement of coercivity in Nd–Fe–B sintered magnets modified by $Pr_{58}Dy_{10}Cu_{32}$ alloy was investigated through scanning electron microscope (SEM) and *in-situ* magneto-optic Kerr effect (MOKE) microscopy. The modification treatment resulted in the formation of a smooth and continuous weakly magnetic grain boundary layer and the $(Nd,Pr,Dy)_2Fe_{14}B$ main phase with a high magnetocrystalline anisotropy field, leading to an increased coercivity of 23 kOe. MOKE observations revealed that the dynamic evolution of the maze domain area under an external magnetic field varied significantly between the original and modified magnets. Compared with the original magnets, the modified magnets exhibited a slower decrease in maze domain area during magnetization and a slower increase during reverse magnetization, contributing to the observed coercivity enhancement.

Keywords: Nd–Fe–B sintered magnets, high coercivity, Pr–Dy–Cu, magnetic domain

PACS: 75.50.–y, 77.80.Dj, 81.05.–t

DOI: 10.1088/1674-1056/adda0c **CSTR:** 32038.14.CPB.adda0c

1. Introduction

The rapid development of high-performance and lightweight intelligent robots urgently requires research and development of rare earth permanent magnetic materials with high magnetic energy product and high thermal stability. Nd–Fe–B sintered magnets have the highest magnetic energy product, but their low coercivity is difficult to meet the above requirements. Overall, improving the coercivity of sintered Nd–Fe–B magnets mainly involves two technical approaches: optimizing their chemical composition and modifying their microstructure. The optimization of their chemical composition is mainly achieved by replacing some of the neodymium elements in the main phase of Nd–Fe–B materials with heavy rare earth elements Dy and Tb,[1,2] improving the anisotropy field of $Nd_2Fe_{14}B$ phase to enhance the coercivity of sintered magnets. The modification of microstructure is mainly accomplished by refining the main phase grains and reducing the content of ferromagnetic elements in the grain boundary phases,[3–8] thereby improving the coercivity of the magnets. The present authors first prepared Dy-free Nd–Fe–B sintered magnets with the coercivity of 20 kOe by the doping of $Pr_{68}Cu_{32}$ eutectic alloy,[9] and since then, many researchers have also conducted further research work on enhancing the coercivity of sintered magnets with other alloys with low melting melting points.[10–20] So far, the vast majority of work has focused on analyzing the reasons for the increase in coercivity by examining the changes in the microstructure of magnets before and after the doping treatment. However, there is limited observation on the magnetic domain structure evolution of magnets before and after the doping treatment with the external applied field, which is very important for learning the causes of coercivity enhancement. Kobayashi only investigated the magnetic domains of sintered magnets after doping with Tb_4O_7 and CaH_2 powders under thermally demagnetized state and saturated magnetization state, but did not observe the dynamic evolution of magnetic domains during magnetization and demagnetization processes.[21] Our collaborator Ming Yue observed magnetic domain variations in sintered magnets under changing external magnetic fields before and after doping with terbium (Tb) nanoparticles.[22] Nevertheless, they did not examine how the modifications of microstructure, especially the composition and morphology of grain boundary phases, affects the evolution of magnetic domains under different ex-

[†]Corresponding author. E-mail: qianhuidong@pku.edu.cn
[‡]Corresponding author. E-mail: hanjingzhi@pku.edu.cn

© 2025 Chinese Physical Society and IOP Publishing Ltd. All rights, including for text and data mining, AI training, and similar technologies, are reserved.

ternal field conditions.

In this work, we introduced the work on enhancing the coercivity of sintered magnets by the combination of altering the intrinsic magnetic properties of $Nd_2Fe_{14}B$ main phase and modifying microstructure of the grain-boundary phase. In order to better understand the contribution of synergetic regulation of main phase and grain boundary phase to the coercivity, we investigated the effect of adding 20 wt.% $Pr_{58}Dy_{10}Cu_{32}$ on the microstructure, magnetism, and magnetic domain structure of sintered magnets. The coercivity of $Nd_{12.2}Pr_{2.6}Fe_{76.3}Co_{2.1}B_{6.0}Nb_{0.2}Al_{0.5}Cu_{0.1}$ sintered magnets reaches 23 kOe after the modification treatment using $Pr_{58}Dy_{10}Cu_{32}$ alloy. The reason for the increase in coercivity will be discussed through microstructural investigation, magnetic measurements and *in-situ* magnetic domain observation with the different magnetic field.

2. Experimental procedure

The Nd–Fe–B raw material in this work is the $Nd_{12.2}Pr_{2.6}Fe_{76.3}Co_{2.1}B_{6.0}Nb_{0.2}Al_{0.5}Cu_{0.1}$ powder with a particle size of about 3.5 μm provided by Advanced Technology & Materials Co., Ltd. The $Pr_{58}Dy_{10}Cu_{32}$ alloy powder is obtained by arc melting the alloy, and then hydrogen decrepitation at 200 °C, and finally mechanical-crushing into fine powders with a size less than 75 μm in an agate mortar. In order to obtain a sintered magnet composed of Nd–Fe–B and Pr-Dy-Cu with a mass ratio of 80:20, it is necessary to first mix Nd–Fe–B powder and Pr–Dy–Cu alloy powder evenly through grinding, then orient and press them into cylindrical "green" compacts under an external magnetic field of 1.5 T and under a pressure of 150 MPa, and finally sinter them at 1050 °C for 5 hours. In order to achieve uniform distribution of rare earth rich grain boundary phases in sintered magnets, the "green" compacts were annealed at 560 °C for 2 hours. Subsequently, the magnetic changes were measured using a *B*–*H* tracer. The changes in the composition and microstructure were examined through scanning electron microscope (SEM), energy dispersive x-ray analysis (EDAX) and electron probe microanalyzer (EPMA). The changes in the magnetic domain structure were observed using magneto-optic Kerr effect microscopy (MOKE, BH-786IP-PK), and the observing plane is perpendicular to the *c*-axis.

3. Results and discussion

We first investigated the effect of Pr–Dy–Cu alloy modification on the magnetic properties of sintered magnets, as shown in Fig. 1. It can be seen that the coercivity of the original magnets before the modification is about 14 kOe; after the modification, the coercivity of the magnets increased to about 23 kOe. This result indicates that adding Pr–Dy–Cu alloy during the preparation of sintered magnets does indeed help improve the coercivity of the magnets, but the increase in coercivity comes at the cost of sacrificing remanence. Thus, for seeking high coercivity and remanence, it is necessary to decrease the amount of Pr–Dy–Cu alloy.[11] However, the slightly excessive addition of Pr–Dy–Cu alloy can help us compare the changes of microstructure and magnetic domain structure before and after the modification, and learn the factors that truly improve the coercivity of the magnets.

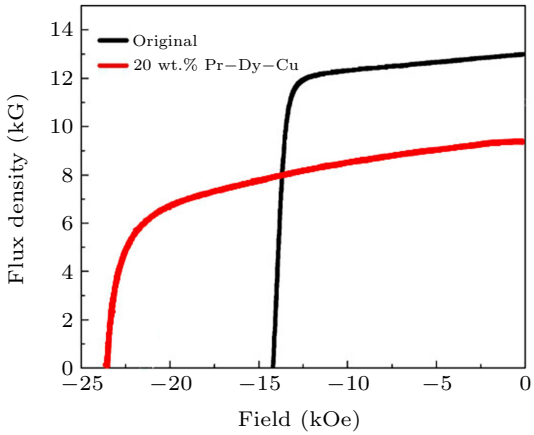


Fig. 1. Demagnetization curves of sintered magnets before and after the modification of Pr–Dy–Cu alloy.

To analyze the reason of coercivity improving, composition and microstructure of sintered magnets before and after the modification were investigated through SEM and EPMA. It is seen in Fig. 2 that the grain size of the main phase remained basically unchanged. In addition, the grain boundary layer of the original sintered magnets was thin and discontinuous, while the grain boundary layer of sintered magnets not only became thicker but also became continuous in most areas after the modification.

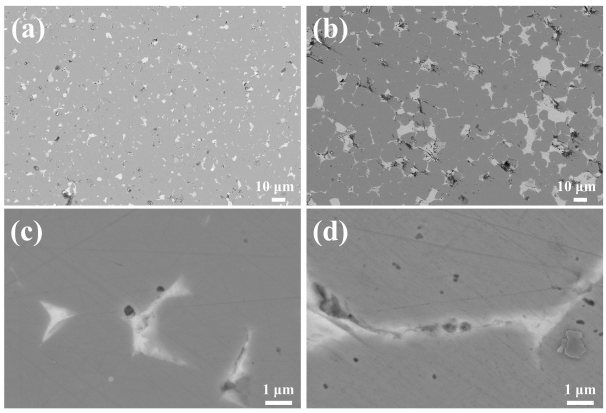


Fig. 2. SEM images of sintered magnets (a) before and (b) after the modification treatment using 20 wt.% Pr–Dy–Cu alloy, (c) and (d) are the enlarged images of the grain boundary of sintered magnets before and after the modification treatment.

Figure 3 shows the area scanning analysis results of various elements in the modified magnets through EPMA. It can be seen that after the modification of the alloy, Pr and

Cu elements mainly enter the rare earth rich grain boundary layer, resulting in a decrease in the iron content in the layer. The Dy element mainly enters the main phase and forms $(Nd,Pr,Dy)_2Fe_{14}B$ phase, which can be confirmed by subsequent magnetic domain observations. It is also seen that there is more Dy content on the grain's edge than in its center, while the content of Nd in the grain's center is higher than that on its edge. According to the gradient distributions of both Dy and Nd elements, it can be inferred that Dy diffused into the grains and displaced some of the Nd element in the $Nd_2Fe_{14}B$ main phases, leading to the formation of $(Nd,Pr,Dy)_2Fe_{14}B$ phase and core–shell structure.

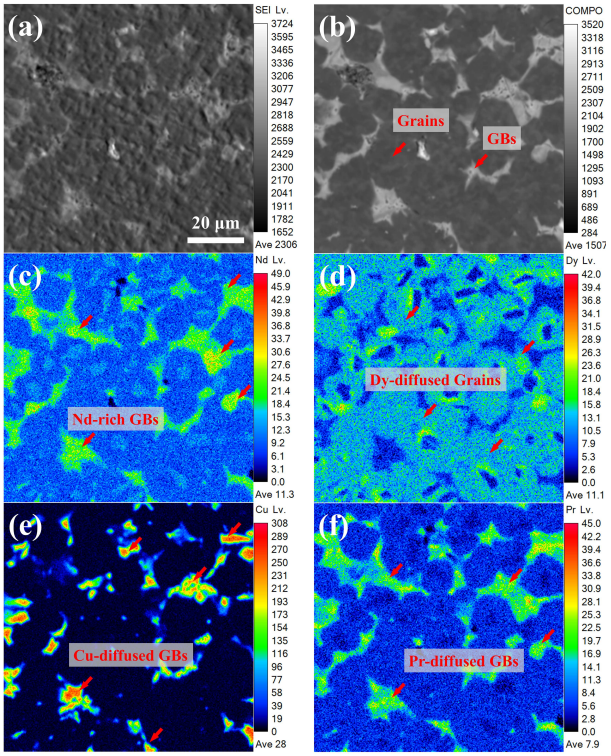


Fig. 3. (a) and (b) Secondary electron imaging (SEI) and composition image of sintered magnets after the modification treatment, and the corresponding electron probe micro analyzer (EPMA) elemental mapping for (c) Nd, (d) Dy, (e) Cu and (e) Pr elements.

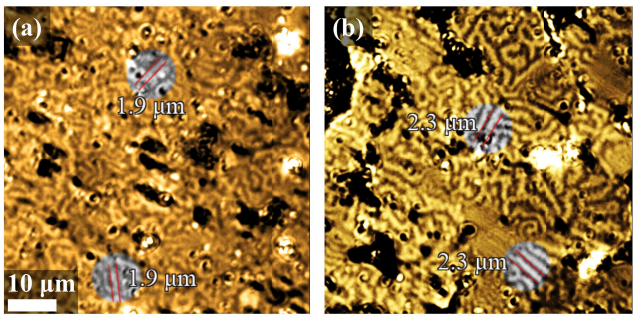


Fig. 4. Magnetic domains of the thermally demagnetized state of the sintered magnets (a) before and (b) after the modification treatment. The observing plane is perpendicular to the *c*-axis.

Figure 4 shows the changes in magnetic domains of the sintered magnets before and after the modification. It can be seen that after the modification of Pr–Dy–Cu alloy, the magnetic domains of the magnets change from blurry to clear and visible, and the magnetic domain width increases. This is because Dy diffused into the main phase, forming the $Dy_2Fe_{14}B$ phase. It has been shown that the magnetic domain width (W) is positively correlated with the magneto-crystalline anisotropy constant K.[21] Due to the higher anisotropy constant of $Dy_2Fe_{14}B$ phase compared to $Nd_2Fe_{14}B$ phase, the magnetic domain width increases after the modification treatment.

In addition, it can also be seen that due to the high content of ferromagnetic elements in the thin grain boundary layer, there is a strong exchange coupling effect between the grains of the original sintered magnets, resulting in a magnetic domain containing several grains. However, after the modification treatment, the content of ferromagnetic elements in the grain boundary layer of the sintered magnets decreases and the thickness of the grain boundary layer increases, and the coupling effect between grains weakens, resulting in isolated magnetic domains for each grain.

In order to further analyze the reasons for the increase in coercivity of sintered magnets after the modification of Pr–Dy–Cu alloy, we investigated the magnetic domain changes during the magnetization and reverse magnetization processes of the magnets before and after modification treatment *in-situ*, as seen in Figs. 5 and 6.

From Figs. 4–6, it can be seen that when the magnets are in a thermally demagnetized state, the magnetic domain state of all grains in the magnets exhibits multi-domain structure like a maze domain. When the magnets are in a magnetization saturation state, the magnetic domain state of all grains appears as a single domain, and the maze domain disappears at this time. When the magnets are in a remanent state, some grains exhibit a single domain state, while others exhibit a multi domain state. Therefore, we can determine the difficulty of magnetization and reverse magnetization of a magnet based on the size of the maze domain area (or multiple domains) under different external magnetic field conditions. The higher the coercivity of a magnet, the slower the maze domain area decreases when transitioning from the demagnetized state to the saturated state, and the slower it increases when transitioning back from the saturated state to the demagnetized state.

For the magnetization process, under the condition of the same external magnetic field of 6000 Oe, there are still a large number of maze domains in the modified magnets, while there are fewer maze domains in the corresponding original magnets. This indicates that the modified magnets are more difficult to magnetize due to its higher coercivity caused by the formation of $(Nd,Pr,Dy)_2Fe_{14}B$ and the modified grain boundary layer.

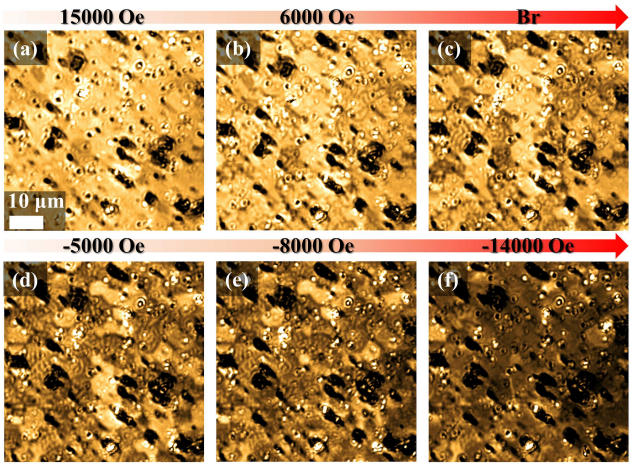


Fig. 5. Magnetic domain evolutions of the original sintered magnets under various magnetic fields.

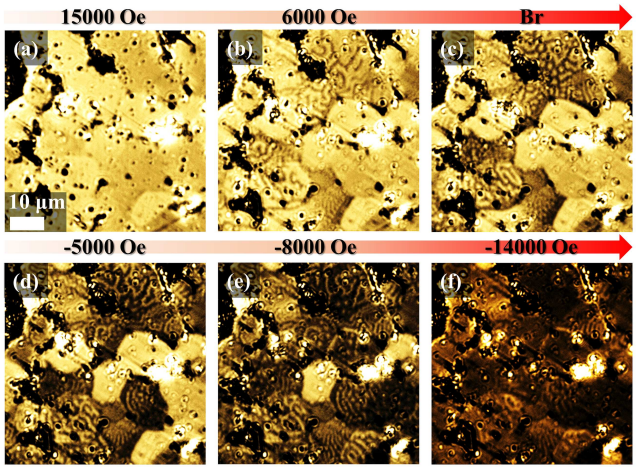


Fig. 6. Magnetic domain evolutions of the modified sintered magnets under various magnetic fields.

In the case of the reverse magnetization process, on the other hand, when the reverse magnetic field gradually increases, such as gradually increasing to −5000 Oe and −8000 Oe, both the modified magnets and the original magnets are in the process of transitioning from the remanent state to the demagnetized state. The modified magnets have fewer maze domains, indicating that it is difficult to form reverse domains, and thus the modified magnets have a higher coercivity. When the reverse magnetization reaches 14000 Oe, which is close to the coercivity (14 kOe) of the original magnets, but lower than the coercivity (23 kOe) of the modified magnets, the modified magnets exhibit bright contrast single domains and maze domains, indicating that it still has a greater number of positive domains, and the overall magnetization remains positive. In contrast, the original magnets show dark contrast single domains and maze domains, indicating that the original magnets have a greater number of reverse domains at this point, manifesting as a negative magnetization. These are consistent with the coercivity characteristics of the two types of magnets. It is notable that due to the damage and oxidation of the Nd–Fe–B magnets' surface during mechanical cutting and grinding processes, the surface coercivity is lower than the overall coercivity of the magnets. The signals of MOKE come from the magnets' surface. Therefore, a reverse magnetic field lower than the coercivity of the magnets can cause the positive domains to reverse.

The above results show that the synergetic modification of Pr, Dy and Cu precisely regulates the structure and magnetism of grain boundary phases, as well as the formation of $(Nd,Pr,Dy)_2Fe_{14}B$ main phases, reducing the possibility of reverse domain nucleation in sintered magnets or increasing the energy of reverse nucleation, thus improving the coercivity of the magnets.

4. Conclusion

In conclusion, the coercivity enhancement is related to the synergetic modification of the grain boundary layers and the main phases. In the original magnets, there exists exchange interaction among the grains due to the thin ferromagnetic grain boundary. However, after the modification, thick and less ferromagnetic boundary layers are induced and grains are largely decoupled. The maze domain area of magnets with different coercivity will exhibit different rates of change with the external magnetic field. The modified magnets show the slower decrease of the maze domain area during the magnetization and the slower increase during the process of reverse magnetization. Hence, a high coercivity is obtained in the modified sintered magnets.

Acknowledgments

Project supported by the National Key Research and Development Program of China (Grant Nos. 2021YFB3500300, 2023YFB3507000, and 2023XYJG0001-01-03), the National Natural Science Foundation of China (Grant No. 52171167), and Inner Mongolia Northern Rare Earth Advanced Materials Technology Innovation Co., Ltd. Project (Grant No. CXZX-B-202304-0004).

References

[1] Hirosawa S, Matsuura Y, Yamamoto H, Fujimura S, Sagawa M and Yamauchi H 1986 *J. Appl. Phys.* **59** 873
[2] Boltich E, Oswald E, Huang M, Hirosawa S, Wallace W and Burzo E 1985 *J. Appl. Phys.* **57** 4106
[3] Sagawa M, Fujimura S, Togawa N, Yamamoto H and Matsuura Y 1984 *J. Appl. Phys.* **55** 2083
[4] Vial J F, Nevalainen E, Sagawa M, Hiraga K and Park K 2002 *J. Magn. Magn. Mater.* **242** 1329
[5] Ramesh R, Thomas G and Ma B M 1988 *J. Appl. Phys.* **64** 6416
[6] Ramesh R and Srikrishna K 1988 *J. Appl. Phys.* **64** 6406
[7] Sepehri-Amin H, Une Y, Ohkubo T, Hono K and Sagawa M 2011 *Scr. Mater.* **65** 396
[8] Sepehri-Amin H, Ohkubo T, Shima T and Hono K 2012 *Acta Mater.* **60** 819
[9] Wan F M, Zhang Y F, Han J Z, Liu S Q, Liu T, Zhou L, Fu J B, Zhou D, Zhang X D, Yang J B, Yang Y C, Chen J and Deng Z W 2014 *J. Appl. Phys.* **115** 203910

[10] Chen G X, Bao X Q, Lu K C, Lv X K, Ding Y, Zhang M, Wang C G and Gao X X 2019 *J. Magn. Magn. Mater.* **477** 17
[11] Zhang Y J, Ma T Y, Liu X L, Liu P, Jin J Y, Zou J D and Yan M 2016 *J. Magn. Magn. Mater.* **399** 159
[12] Bu M F, Ren S Q, Xin B and Yan M 2023 *Intermetallics* **157** 107891
[13] Bao X Q, Wang Z H, Zhang S J, Li J H and Gao X X 2024 *J. Magn. Magn. Mater.* **591** 171725
[14] Wang X, Zhu M G, Xia F, Zhang M L, Liu F, Guo Y J, Zhang L L, Zhang G R and Li W 2021 *J. Rare Earth.* **39** 979
[15] Tang W, Wang J, Pan C C, Kang M C, Zhou L, Kramer M J, Cui J, and Anderson I E 2024 *IEEE Trans. Magn.* **60** 2100505
[16] Yu Z G, Chen S Y, Zeng C C, Yu H Y, Wu Y X, He J Y and Liu Z W 2024 *J. Mater. Chem. C* **12** 15239
[17] Yu Z G, Liu X Y, He J Y, Cao J L, Fan W B, Wu Y X, Yu H Y, Liu Z W, Wang Z and Niu E 2023 *J. Mater. Chem. C* **11** 645
[18] Wong Y J, Chang H W, Lee Y, Chang W C, Chiu C H and Mo C C 2022 *IEEE Trans. Magn.* **58** 2102305
[19] Lv M, Kong T, Zhang W H, Zhu M Y, Jin H M, Li W X and Li Y 2021 *J. Magn. Magn. Mater.* **517** 167278
[20] Hirosawa S 2019 *IEEE Trans. Magn.* **55** 2100506
[21] Kobayashi K, Urushibata K, Matsushita T, Sakamoto S and Suzuki S 2014 *J. Alloys Compd.* **615** 569
[22] Ji M, Wang Z J, Liu W Q, Li Y Q, Chen H, Wu H H, Du R H, Zhang D T, Yue M, Yi X F, Liu Y H and Zha S S 2024 *J. Alloys Compd.* **970** 172598